

EXPERIMENTAL INVESTIGATION OF A TACTILE SENSOR BASED ON BENDING LOSSES IN FIBER OPTICS

John G. Winger and Kok-Meng Lee

Georgia Institute of Technology
The George W. Woodruff School of Mechanical Engineering
Atlanta, GA 30332

ABSTRACT

Sensory feedback will be necessary in the next generation of robots if true flexible automation is to be achieved. One form of sensory feedback is tactile sensing. Tactile sensing, or taction, is the continuously variable sensing of forces and force gradients over an area. Problems such as hysteresis, limited range and sensitivity, and high cost have victimized many of past approaches to taction. Therefore, this paper presents experimental results of an investigation of a prototype tactile sensor design based on microbending losses in fiber optics. In particular, the parameters which determine the sensitivity of a fiber to bending losses were identified, experiments were performed on a multimode optical fiber, and a prototype tactile sensor was constructed and tested. Results indicate that the limiting factor on the performance of the tactile sensor was the visco-elastic behavior of the fiber's cladding.

1. INTRODUCTION

By definition, tactile sensing (or taction) is the continuously variable sensing of forces and force gradients over an area. This task is usually performed by an array of individual sensors called forcels. By considering the outputs from all of the individual forcels, it is possible to reconstruct a tactile image of the targeted object. This ability is a form of sensory feedback which is important in the development of robots intended to be used in flexible automation applications. By using the tactile image of the grasped object, it will be possible to determine such factors as the presence, shape and texture of the grasped part. The location and orientation of the object as well as reaction forces and moments could be detected. Finally, the tactile image could be used to detect the onset of part slipping.

A review of past investigations has shown that a tactile sensor intended for industrial use should have the following characteristics. Most importantly, the response of the individual forcels should be repeatable and free from hysteresis. The forcels should be capable of detecting loads ranging from 0 to 1000 grams, have a 1 gram sensitivity¹ and a speed of response of approximately 10 milliseconds².

Furthermore, forcels should be spaced about 2mm apart³ and in at least a 10x10 grid⁴. Using these performance criterion as a general guideline, the potential of a tactile sensor based on bending losses in fiber optics was investigated.

Tactile sensors which utilize optical fibers are of particular interest due to the following advantages: low cost, increased sensitivity, immune to adverse electromagnetic interference, large bandwidth and high data rates, compatible with fiber telemetry and geometrical versatility⁵. A high resolution tactile sensor, which utilizes fibre optics to transmit the tactile image to a standard television camera for digital processing, was developed at MIT⁴. A second type of tactile sensor, commercially available from Tactile Robotic Systems (Sunnyvale, CA), operates by detecting the amount of light coupled between source and detector fiber pairs. Applied loading causes relative motion between the fibers resulting in light attenuation⁴. Recently, another tactile sensor design based on monitoring the amount of optical coupling between two fibers was reported⁶. The tactile sensor design presented in this paper is based on the modulation of light propagating through a fiber due to microbending. The concept of monitoring light losses due to microbending has been used in displacement sensors^{7,8}, a hydrophone⁹, a pressure sensor¹⁰ and was suggested for consideration of a tactile sensor design¹¹.

This paper presents the results of an experimental investigation of a tactile sensor design based on microbending effects in fiber optics. The fiber parameters which are the most appropriate for the tactile sensor design are identified. A number of experiments, which were performed on the chosen fiber to determine the linearity, repeatability, response time and stability of light attenuation for a constant fiber deformation, are presented. The experimental data provide a rational basis for a prototype design.

2. PARAMETERS INFLUENCING MICROBEND LOSSES

Optical fibers are a type of dielectric waveguide. These waveguides channel light energy by "trapping" it

between cylindrical layers of dielectric materials. In the most simple case, the fiber's glass core is surrounded by a cladding which has a larger refractive index.

In an ideal straight fiber, there are a finite number of modes or ray paths in which light can propagate. These modes represent allowable eigensolutions of the source-free, steady-state Maxwell equations and are therefore called bound or guided modes. Radiation modes, on the contrary, are unstable solutions to Maxwell's equations. These modes quickly lose light through radiation of energy out of the fiber's core. In the microbending process, light is lost from the core of a fiber when a mechanical bend or perturbation results in coupling between guided and radiation modes. Regardless of the type of fiber, there are no bound rays in the bent region. Instead, every ray which was previously bound on the straight section of fiber must radiate some of its energy¹². How much power is lost depends on fiber parameters as well as the radius of curvature and spatial frequency of the bend. These factors will be briefly discussed so that the proper fiber parameters may be identified.

2.1 Single versus Multimode Fibers In general, optical fibers may be classified as either single mode or multimode fibers. As the name implies, a single mode fiber can support only one mode or ray path (actually two polarization states of a single fundamental mode) while multimode fibers are capable of transmitting many modes. Single mode fibers are harder to splice together and are much more sensitive to alignment errors between the light source and the fiber. Most importantly in the tactile sensor application, single mode fibers are less sensitive to bending. Since we plan on bending a fiber and monitoring the resulting attenuation of light energy, it is to our advantage to use multimode fibers.

2.2 Weakly Guiding Fibers

The weakly guiding designation refers to a fiber which has a relatively small difference between the maximum core and cladding refractive indices¹³. The bound rays which do exist are more susceptible to coupling with refracted rays due to bends and perturbations in the fiber (microbend losses). Since a weakly guiding fiber provides less guidance, it is more susceptible to losses due to fiber perturbations. Thus for the tactile sensor application, a weakly guiding fiber is the most appropriate choice since we desire maximum susceptibility to microbends.

2.3 Core-Cladding Coupling Conditions

Optical fibers can have either step or graded refractive index profiles. Fibers with step profiles have refractive indices which are constant across the cross-section of the core. Graded profile fibers, on the other hand, have refractive indices which are a function of the radial distance from the core's axis. In order to understand which type of fiber is the most sensitive to bending losses, the

dependence of light loss to the spatial frequency of the disturbance must be illustrated.

Coupling occurs in a bent fiber when the wave number ($k = 2\pi/\Lambda$) of the mechanical distortion equals the difference in the propagation constant between adjacent modes. This may be written explicitly in the following manner¹⁵.

$$\beta_{j+1} - \beta_j = \frac{2\pi}{\Lambda} \quad (1)$$

β_{j+1} and β_j represent adjacent longitudinal propagation constants and Λ is the mechanical wavelength of the periodic fiber distortion. It can be shown that the difference between adjacent modes is given by⁹:

$$\beta_{m+1} - \beta_m = \left(\frac{\alpha}{\alpha+2} \right) \frac{2\sqrt{\Delta}}{\rho} \left(\frac{m}{M} \right)^{(\alpha-2)/(\alpha+2)} \quad (2)$$

where

- m - is the mode number
- M - total number of guided modes
- α - a constant which describes the index profile
- Δ - describes difference between core and cladding refractive indices
- ρ - core radius

Setting Equation (1) equal to Equation (2), this results in the following equation for a fiber with a parabolic refractive index profile ($\alpha=2$), :

$$\delta\beta = \beta_{m+1} - \beta_m = \frac{\Delta^{0.5}}{\rho} \quad (3)$$

As this relation illustrates, multimode fibers with parabolic profiles ($\alpha=2$) have allowable modes of propagation spaced equally apart in k space. This equal spacing is important, since it means that there exists an optimal mechanical wavelength which results in the most efficient coupling between adjacent modes. Furthermore, this wavelength is the same for every pair of adjacent modes, resulting not only in the coupling of the highest order propagation mode to the first radiation mode, but a linkage between all modes. Therefore, graded index, multimode fibers with profiles which are approximately parabolic are much more sensitive than step profile fibers to microbends.

3. FIBER OPTIC MICROBEND EXPERIMENT

Once the important fiber parameters were identified, the behavior of the fiber under bending was analyzed experimentally. This experimentation was performed in order to determine the following factors which were considered critical in the design of a fiber optic based tactile sensor: (1) linearity of the attenuation of light with

respect to fiber deformation; (2) repeatability of the light attenuation; (3) stability or time invariance of the light attenuation for a constant fiber deformation; (4) dependence of the attenuation on the spatial period of the fiber deformer; (5) the effect of multiple bends on a single fiber; and (6) time required to reach a steady state output irradiance for a step input displacement (speed of response). These factors were analyzed by monitoring the irradiance of the light propagating through a fiber while applying a controlled deformation.

3.1 Equipment

The experiment consisted of a light source, a multimode optical fiber, a method of coupling light to the fiber, mode strippers, a method of suppressing the higher order lossy modes which are present in the transition region of a short fiber, a controlled and repeatable method of deforming the fiber, and a detector and its supporting circuitry. A schematic of this equipment is presented in Fig. 1. The fiber used in the experiment was a multimode fiber supplied by AT&T Bell Labs (Norcross, Georgia). The fiber is multimoded ($V=48.5$), has a refractive index which is approximately parabolic ($\alpha=2.13$), is weakly guiding ($\Delta=0.0094$), and has a core diameter of $49\ \mu\text{m}$ and a cladding diameter of $125\ \mu\text{m}$. A Helium-Neon laser was used as a light source.

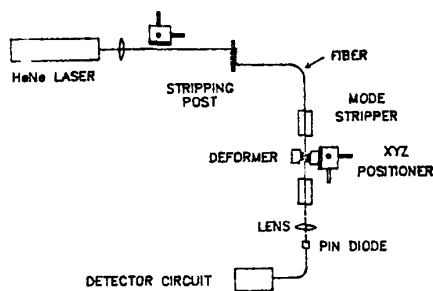


Figure 1 Schematic of the Experiment Setup

When light is coupled into an optical fiber, many modes are excited. These include both bound and refracted modes. For an ideal, straight fiber made of a lossless, dispersionless dielectric material, the amount of power guided by the bound modes should remain constant. This, however, is not the case for the radiation modes which decay along the length of the fiber. Therefore, it is reasonable to assume that the fiber can be separated into two regions: the spatial transient and the spatial steady state. The length of the spatial transient region is defined to be the distance at which radiation modes have disappeared to first order. This condition is dependent on the waveguide parameter, V . For multimode fibers with large waveguide parameters, such as the fiber under consideration, lengths of 500 meters or more may be required before a type of radiation mode, called tunneling modes, has sufficiently decayed¹⁴. Fortunately, it has been

shown that the rate of tunneling mode attenuation in multimode fibers can be greatly increased by inducing perturbations along the fiber¹⁵. One method of easily achieving this goal in experimental situations has been to wrap the fiber around a 3/8th inch dowel a couple of times¹⁶. This procedure artificially shortened the length of the spatial transient region which allowed reasonable lengths of fiber to be used.

Data was taken for various types of deformers. For each deformer type, the following procedure was utilized. The active deformer was positioned so the fiber was just touching the teeth of both deformers. The fiber deflection was then incremented by $0.0127\ \text{mm}$ ($0.0005\ \text{in}$) and 25 more readings were taken. This procedure was repeated until the fiber output reached around ten percent of the undeflected output which usually occurred somewhere around $0.178\ \text{mm}$ ($0.007\ \text{in}$) of deflection.

3.2 Experimental Results

One of the primary goals of this experiment was to investigate the repeatability of the attenuation of light propagating through a fiber optic when the fiber is deformed. Throughout the experiment there was a region from the zero deflection point out to around 0.004 inches of deflection where the output exhibited unrepeatable, nonlinear behavior. It was possible to see some light leaving the fiber in the deformed region for this range of deflections, however, the loss of light was not detected by the photodetector which was operating in a bright field mode. That is, the detector was situated at the end of the fiber where it could monitor the amount of light remaining in the fiber. A dark field arrangement, where the light escaping from the bent region of the fiber is monitored, probably would have been capable of detecting light attenuations due to small deflections. However, the bright field detection method was used, since it is easier to perform and does not require the detectors to be placed adjacent to the bent region of the fiber.

For deflections larger than $0.102\ \text{mm}$ ($0.004\ \text{in}$), it was possible to show that the light propagating through the fiber was attenuated in a linear manner. As was mentioned previously, meta-stable tunneling modes exist in the spatial transition region and were suppressed by wrapping the fiber around a $9.5\ \text{mm}$ ($3/8\ \text{in}$) dowel for a couple of revolutions. This resulted in a drastic increase in repeatability between experimental runs. This result can be readily observed in the plots of the experimental runs presented in Figure 2. With no dowel used to strip the fiber of leaky modes, the rate of attenuation with respect to fiber deflection (slope) for the first and second runs are considerably different. The repeatability of the results can be significantly improved by stripping out the tunneling modes. Figure 2 is also a good illustration of the unstable region which typically occurs between zero and $0.102\ \text{mm}$ ($0.004\ \text{in}$) of deflection.

By engaging more than one set of deformer teeth, it was possible to simulate a number of forcels directly adjacent to each other. This arrangement was accomplished by using the XYZ positioner to move the active deformer such that the desired number of teeth meshed. Each tooth on the active deformer, which correspond to individual forcels, could not be deflected independently of each other. However, if the attenuation rate were truly a linear function of the number of teeth engaged, one would expect to have twice the attenuation when two teeth were engaged compared to one. This experiment was run using one to seven sets of engaged deformer teeth with each case run at least twice to insure the data was repeatable. The results for one to three teeth are plotted in Figure 3 and clearly indicate that increasing the number of teeth engaged had no effect on the output. This is an important results since it means that each fiber may only be deformed by a single forcел. As a result, one would be required to use 64 individual fibers to form an eight by eight grid of forcels instead of the 16 which would be needed if this restriction did not apply. The implications of this fact are now a fiber, source, and detector will be required for each individual forcел. This will increase the hardware cost per forcел. However, it also corresponds to a decrease in the level of logic that would be required to interpret the sensor's output.

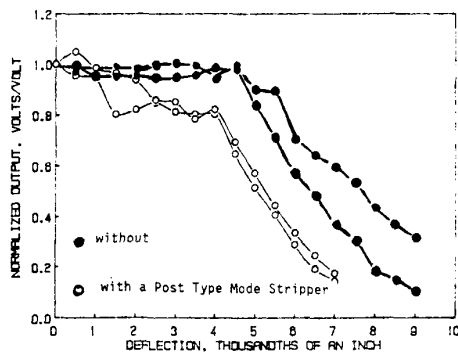


Figure 2 Effect of Post Type Mode-Stripper on Repeatability

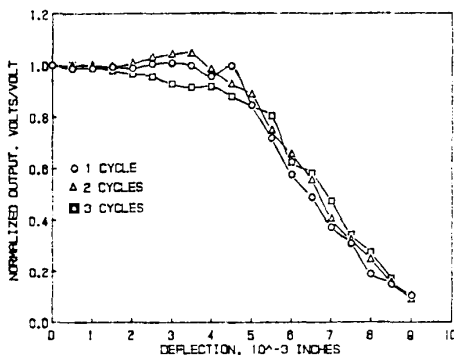


Figure 3 Attenuation Curves for 1, 2, and 3 Cycles of Deflection

A number of different types of deformer materials were tried, as well as deformers which had different mechanical wavelengths. It was determined experimentally a critical deformer wavelength for the fiber used in the experiments was 1.53 mm.

4. TACTILE SENSOR DESIGN

It was possible to divide the design of the tactile sensor into two separate portions. This natural division is expressed in Equation (4), which describes the sensitivity of an individual forcел. This

$$\frac{\Delta T}{\Delta F} = \left(\frac{\Delta T}{\Delta X} \right) \left(\frac{\Delta X}{\Delta F} \right) \quad (4)$$

relation indicates that the sensitivity to external loads ($\Delta T/\Delta F$) is the product of the sensitivity of the fiber to displacements ($\Delta T/\Delta X$) and the compliance of the sensor's surface ($\Delta X/\Delta F$). The design of the sensor such that fiber bending is achieved in the most efficient manner possible (maximum $\Delta T/\Delta X$) and still incorporates all the critical parameters identified in the previous two chapters is the more complex of the two problems. Furthermore, investigations into what characteristics are the most desirable for gripping surfaces have already been performed. Therefore, the portion of the sensor design concerned with the modulation of fiber bending will be the area of primary concern.

4.1 Hardware Design

Each forcел consisted of a section of fiber sandwiched between an active and passive deformer. The passive side was the saw-tooth pattern, $\lambda = 1.53$ mm, and the active portion was a piece of steel wire which was glued to the bottom of the compliant surface of the sensor. This configuration is illustrated in Figure 4.

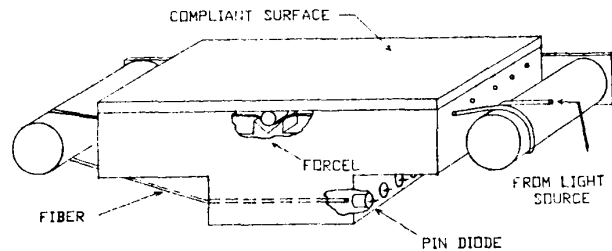


Figure 4 Schematic of Prototype Tactile Sensor

For the purposes of testing the tactile sensor design in laboratory conditions, it was considered appropriate to use a Helium-Neon laser as a light source for a 2x2 array sensor. As was the case in the bending experiment, the photodetectors were operated in a bright field mode due to the inherent simplicity of bright field detection and the option of remotely positioning the PIN diodes. Each fiber was wrapped around a 13 mm diameter dowel a few times before entering the sensing region to attenuate the marginally stable tunnelling modes present in the spatial transition regions of all fibers, which served as a post-type mode stripper.

On initial consideration, one might think that a more exotic material would be required for the sensor surface. However, studies have shown that inner-tube rubber performs well as a gripping surface under both dry and slippery conditions¹⁷. Furthermore, this material is readily available, inexpensive, easy to work with, and has a Modulus of Elasticity of 6.7×10^{-3} Pa (46.4 psi).

The output of the four PIN diodes was amplified by a simple operational amplifier circuit before being read using an IBM XT equipped with a Dash 16F analog to digital data acquisition board. It was determined that the sensor's output contained an AC component which was filtered out. The photodetector output remained fairly constant with a standard deviation of 0.004 volts once the laser had thermally stabilized.

4.2 Prototype Evaluation

The tactile sensor design was tested in order to determine its ability to detect tactile information. A number of experiments were performed which were intended to explore such characteristics as the repeatability of the sensor's output, the sensitivity and range of each of the forcels, and the sensor's spatial resolution. The results of the experimental evaluation are summarized as follows.

Repeatability The repeatability of the output was tested using a weight of 200 grams which was placed or removed manually on the sensor's surface at every fifteen or twenty minutes. The output levels were 0.5064, 0.5072, and 0.5085 volts with the weight removed. This high level of repeatability for the no load condition was typical for moderate loading. However, with the weight applied, the output were 0.4441, 0.4951, and 0.4518 volts which were not quite as consistent. This decrease in repeatability could have been influenced by the experimental procedure used. It was assumed that the weight was large enough so that placement would not be critical. This assumption was probably not entirely sound since there was some curvature to the sensor's surface. Small variations in the position of the weight could have resulted in differences in the load that the forcel "saw" resulting in a decrease in repeatability.

Next the loading curve for an individual forcel was determined experimentally using a point load which made it possible for all the loads to be placed in exactly the same position while maintaining a constant area of contact (92.9 mm^2). The results obtained using this procedure are presented in Figure 5, which is a plot of the normalized output voltage versus the total applied load for one of the forcels. Again, the response in the region from 125 to 225 grams is approximately linear. Furthermore, in the linear region of the curve (between 125 and 225 grams), the sensor was capable of detecting 5 gram variations in the applied loading.

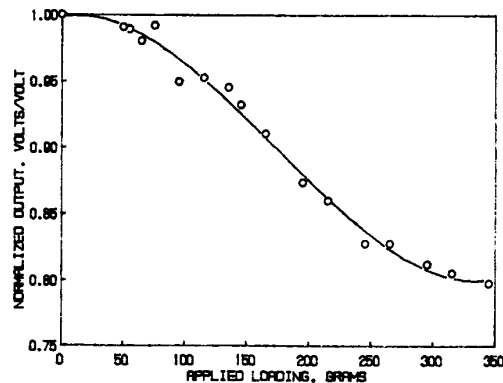


Figure 5 Loading Response of a Forcel

Hysteresis The biggest problem with the microbending based tactile sensor was the amount of hysteresis encountered. Since the cladding of the fiber was made of a visco-elastic material, some hysteresis was expected. In order to determine how much hysteresis existed, the sensor was loaded in 50 gram increments up to 250 grams and then back down to the no applied loading condition. The results for this experiment are plotted in Figure 6. It should be possible to reduce the level of hysteresis down to an acceptable level by coating the fiber in the bent region with an elastic material or a more suitable cladding.

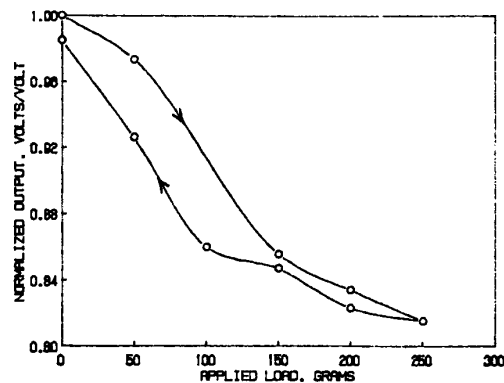


Figure 6 Hysteresis Curve

Speed of Response A step input was approximated by dropping a weight using the point loading device and a trigger circuit. The sensor was determined to have a time constant of 0.14 seconds.

Spatial Resolution The spatial resolution of the sensor was investigated by monitoring the output of the forceps while varying the position of a constant point load. A grid of loading points was laid out on the sensor's surface and the loading bar was positioned over these points manually. 1.27 mm (0.05 in) variations in the point of loading resulted in discernible changes in the sensor's output. Since the amount of spatial resolution obtainable for a given tactile sensor is heavily dependent on the compliance of the sensor's surface, no attempt was made to determine the lower limit of the resolution.

Cross Talk In order to determine if any cross talk existed between fibers, one of the fibers was excited by the laser while the output of the other three fibers was monitored. No cross talk was detected. This result was expected, since the light radiating from the excited fiber was diffuse and had little chance of becoming coupled into the other fibers.

5. CONCLUSIONS

An experimental investigation of a prototype tactile sensor based on microbending losses in fiber optics has been performed. The parameters which determine the sensitivity of a fiber to bending losses were identified. A weakly guiding, multimode fiber with a parabolic refractive index profile was tested. Experiments performed on this fiber indicated that the attenuation of light with respect to fiber deflection was approximately linear and repeatable. The linear portion of the curve occurred between by 0.102 mm and 0.178 mm and was preceded and followed by nonlinear regions. Experimentation indicated that consecutive bends did not increase the rate of light attenuation. Therefore, a fiber will be required for each individual forceps.

Repeatability tests performed on a 2x2 prototype tactile sensor indicated that the forceps could reliably detect a cycled load. The sensor was also found to have a time constant of 0.14 seconds. The most severe problem encountered was the amount of hysteresis present which was due to the visco-elastic nature of the fiber's cladding. The hysteresis also limits the amount of sensitivity and range attainable. Possible solutions to this problem include coating the fiber with an elastic material or using a fiber with a cladding which possesses the appropriate mechanical properties.

ACKNOWLEDGEMENT

The authors would thank Dr. R. J. Ritger for his discussions and the contribution of AT&T fibre. The

research was supported by the General Fund of the George W. Woodruff School of Mechanical Engineering at Georgia Tech.

BIBLIOGRAPHY

1. Hollerbach, J. M. "Workshop on the Design and Control of Dexterous Hands", April 1982, Memo No 661, MIT - AI Laboratory.
2. Harmon, L. D. "Automated Tactile Sensing", The Int. J. of Robotics Research, Vol. 1, No 2, Summer 1982, pp 3-32.
3. Dario, P. and De Rossi, D. "Tactile Sensors and the Gripping Challenge", IEEE Spectrum, August 1985, pp 46-52.
4. Ogorek, M. "Tactile Sensors", Manufacturing Engineering, Feb. 1985, pp 69-77.
5. Montgomery, J. D. and Glasco, J. "Fiber Optic Sensor Long-Range Market Forecast", Fiber Optic Sensors, SPIE Vol 586, 1985.
6. Schoenwald, J. S.; Thiele, Alfred W.; and Gjellum, David E. "A Novel Fiber Optic Tactile Array Sensor", Proc. of the IEEE Int. Con. on Robotics and Automation, 1987, pp 1792-1796.
7. Krieh, M.; Steijer, O.; Pers, O.; and Edwall, G. "Fibre-Optic Dark-Field Micro-Bend Sensor", Fiber Optic Sensors, Vol 586, SPIE - The International Society for Optical Engineers, 1985, pp 216-222.
8. Lagakos, N.; Litovitz, T.; Macedo, P.; Mohr, R.; and Meister, R. "Multimode Optical Fiber Displacement Sensor", Applied Optics, Vol 20, No 2, January 1981, pp 167-168.
9. Lagakos, N.; Trott, W.J.; Hickman, T.R.; Cole, J. H.; and Bucaro, J. A., "Microbend Fiber-Optic Sensor as Extended Hydrophone", IEEE J. of Quantum Electronics, Vol QE-18, No. 10, October 1982, pp 1633-1638.
10. Fields, J. N.; Asawia, C. K.; Ramer, O. G. and Barnoski M. K.; "Fiber Optic Pressure Sensor," J. Acoust. Soc. Amer. 67, 816 (1980)
11. De Paula, R. P.; and Moore E. L.; "Fiber Optic Sensor Overview," Proceedings of SPIE Vol 566, San Diego, CA 1985.
12. Winkler, C.; Love, J.D. and Ghatak, A.K. "Loss Calculations in Bent Multimode Optical Waveguides", Optical and Quantum Electronics, Vol 11, 1979, pp 173-183.
13. Gloge, D. "Weakly guiding fibers", Applied Optics, Volume 10, No.10, October 1971, pp 2252-2258.
14. Snyder, A. W. and Love, John D. Optical Waveguide Theory. Chapman and Hall, New York, 1983.
15. Olshansky, R., "Propagation in Glass Optical Waveguides", Review of Modern Physics, Vol. 51, No. 2, April 1979, pp 341-365.
16. Ritger, A. J. Informal Discussion at Fiber Tour '87, Atlanta Hyatt Regency, May 6, 1987.
17. Cutkosky, M. R. and Wright, P. K. "Friction, Stability and the Design of Robotic Fingers", The Int. J. of Robotics Research, Vol 5, No 4, Winter 1986.